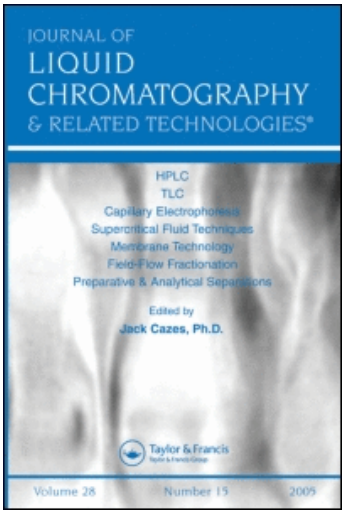

Journal of Liquid Chromatography & Related Technologies
Publication details, including instructions for authors and subscription information:
http://www.informaworld.com/smpp/title~content=t713597273

Experimental Study of Continuous Separation of 1-1'-Bi-2-Naphthol Enantiomers by an Eight-Column Simulated Moving Bed System

Shih-Ming Lai[a]; Rong-Yi Chen[a]
[a] Department of Chemical Engineering, National Yunlin University of Science and Technology, Taiwan, R.O.C

Online publication date: 06 September 2003

To cite this Article Lai, Shih-Ming and Chen, Rong-Yi(2003) 'Experimental Study of Continuous Separation of 1-1'-Bi-2-Naphthol Enantiomers by an Eight-Column Simulated Moving Bed System', Journal of Liquid Chromatography & Related Technologies, 26: 12, 1853 — 1875
To link to this Article: DOI: 10.1081/JLC-120021755
URL: http://dx.doi.org/10.1081/JLC-120021755

JOURNAL OF LIQUID CHROMATOGRAPHY & RELATED TECHNOLOGIES®
Vol. 26, No. 12, pp. 1853–1875, 2003

Experimental Study of Continuous Separation of 1-1′-Bi-2-Naphthol Enantiomers by an Eight-Column Simulated Moving Bed System

Shih-Ming Lai* and Rong-Yi Chen

Department of Chemical Engineering, National Yunlin University of Science and Technology, Taiwan, R.O.C.

ABSTRACT

The separation of 1,1′-bi-2-naphthol racemic mixtures, using the eight-column simulated moving-bed (SMB) method with chiral columns of Pirkle *D*-phenylglycine and each column length of 10 cm, was investigated experimentally in this study. A quick method was used to determine the optimal operating conditions for the SMB system. This was based on the "triangle theory," and good separation conditions were found based on the experimental results of a series of SMB experiments conducted around the complete separation region of the "triangle theory." The optimal operating conditions for each of the solvent composition systems (hexane/IPA = 90/10, 80/20, 70/30) were found, and the effect of solvent compositions on the SMB system performance was studied based on the above quick method. Good system performance (with purity

*Correspondence: Shih-Ming Lai, Department of Chemical Engineering, National Yunlin University of Science and Technology, 123, Sec. 3, University Road, Touliu, Yunlin 640, Taiwan, R.O.C.; E-mail: laism@pine.yuntech.edu.tw.

DOI: 10.1081/JLC-120021755
1082-6076 (Print); 1520-572X (Online)

MARCEL DEKKER, INC.
270 Madison Avenue, New York, New York 10016

and recovery higher than 97% and productivity higher than 0.44 mg/min of each isomer) was achieved using 80/20 hexane/IPA as eluent, which was found to be a suitable solvent composition for our SMB system.

Key Words: Enantiomers; Chiral columns; Simulated moving-bed; Solvent composition; System performance; Optimal operation.

INTRODUCTION

The fundamental work of Broughton and Gerhold[1] led to the use of simulated moving-bed (SMB) chromatography in the petrochemical industry, where several bulk large-scale separations, known as SORBEX processes, have been established. This technology has recently been applied in new areas, such as biotechnology, pharmaceuticals, and fine chemistry.[2] Especially in the pharmaceutical industry, SMB is now considered to be the most promising technique for the preparative production of single enantiomeric drugs, one that is able to compete with previously dominant techniques, such as batch elution chromatography, diastereoisomeric crystallization, and asymmetric synthesis.[3]

When compared with batch elution chromatography, SMB chromatography has the main advantage of being a continuous process able to achieve high purity and recovery for low selectivity separations, along with reductions in eluent consumption and the adsorbent requirements.[4] The concept behind SMB technology is based in the true moving bed (TMB) process, where the liquid goes up and the solid goes down in each zone; then countercurrent contact between the solid and liquid occurs, leading to a high mass transfer driving force [Fig. 1(a)]. The liquid flowing out of section IV is recycled back to section I, while the solid coming out of section I is recycled back to section IV. The feed is continuously injected into the middle of the system, and two product lines can be collected: the extract, which is rich in the more retained species, and the raffinate, which is rich in the less retained species. Unfortunately, the method cannot really be implemented because of operating problems associated with solid circulation in a TMB unit. This is the main reason why an SMB process is preferred. In SMB technology [Fig. 1(b)], the countercurrent movement is simulated by means of an appropriate flow switching sequence: the adsorbent bed is divided into a number of fixed-bed columns, while the inlet (eluent and feed) and outlet (extract and raffinate) lines move simultaneously, one column at fixed switch time intervals in the direction of the fluid phase flow.

To optimally operate an SMB system, a lot of parameters, i.e., the liquid (recycle, feed, eluent, extract, raffinate) and solid (equivalent to the

MARCEL DEKKER, INC.
270 Madison Avenue, New York, New York 10016

(a)

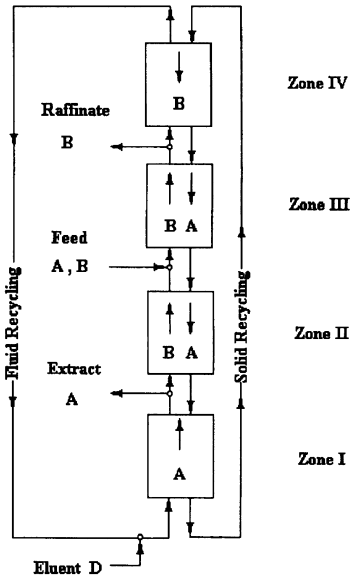

(b)

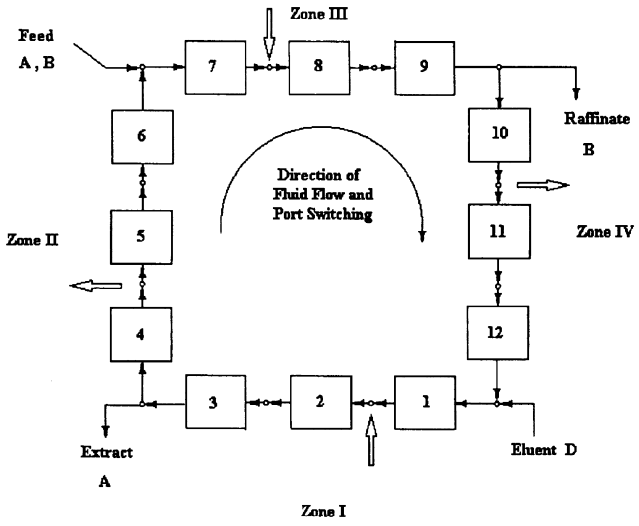

Figure 1. Sketch of the operating schemes: (a) four-section TMB, (b) four-section SMB.

MARCEL DEKKER, INC.
270 Madison Avenue, New York, New York 10016

switch time) flow rates, have to be chosen correctly. Modeling and simulation of the SMB separation processes have received increasing attention because they could lead to significant savings in material and time, as the operating parameters could be determined during the technology development stage. The so-called "triangle theory," based on the TMB approach, provides explicit criteria for choosing the proper operating conditions for both linear and non-linear systems.[5–7] However, it has been developed under ideal conditions (with axial dispersion and mass transfer resistance neglected). When mass-transfer effects are present, there is no explicit expression to define these limits. Azevedo and Rodrigues[8] obtained, through simulation, the new limiting values for the flow-rate constraints in the presence of mass-transfer effects and showed that the complete separation region proposed by the "triangle theory" was considerably reduced. Nevertheless, the reliability of their simulation is based on the accurate adsorption characteristics, including equilibrium and kinetic model parameters.

A quick and straightforward strategy that does not involve complicated mathematical models or tedious measurements of isotherm and kinetic parameters for optimal operation of an SMB system was developed in our previous study.[9] It is based on the "triangle theory," and good separation regions that take non-linear equilibrium and mass-transfer effects into consideration can be found, based on experimental results from a small number of SMB experiments.

In this study, the continuous separation of enantiomers of 1-1′-bi-2-naphthol in the chiral columns of Pirkle covalent *D*-phenylglycine (3,5-dinitrobenzoyl derivative of phenylglycine covalently bonded to aminopropyl silica gel) using an eight-column SMB unit was investigated. Three different solvent composition systems (hexane/IPA = 90/10, 80/20, 70/30) were tested and the operating conditions that lead to optimal system performance for each solvent composition system were found, based on the above quick method.[9] The effect of solvent compositions on the SMB system performance was then studied.

THEORY

Optimal Operation of a Simulated Moving-Bed

There are two main strategies for modeling SMB processes: one is the real SMB model, and the other is the equivalent TMB model. Although small differences exist between these two strategies, the performance of an SMB operation can be predicted and the above operating conditions can be properly selected using the TMB approach.[10]

The design problem of a TMB consists of setting the proper operating conditions (liquid and solid flow rates) needed to obtain the desired separation. In order that the less retained species will move in the direction of the liquid phase and the more retained one in the direction of the solid phase, some constraints have to be satisfied in each column. The constraints, defining a complete separation in a TMB unit for a linear equilibrium binary system in the absence of dispersion and mass-transfer effects, can be expressed as:[11,12]

$$\begin{aligned} &\gamma_{\mathrm{I}} > FK_A;\ FK_B < \gamma_{\mathrm{II}} < FK_A \\ &FK_B < \gamma_{\mathrm{III}} < FK_A;\ \gamma_{\mathrm{IV}} < FK_B \end{aligned} \tag{1}$$

where γ_j is the ratio between the fluid and solid velocities, i.e., $\gamma_j = v_j/u_s$, v_j is the interstitial fluid velocity ($j = \mathrm{I}, \mathrm{II}, \mathrm{III}, \mathrm{IV}$), u_s is the equivalent interstitial solid velocity in the TMB process, K_i is the Henry's constant of the species i ($i = A, B$), $F = (1-\varepsilon)/\varepsilon$ is the phase ratio, and ε is the total column porosity. These constraints are in accordance with the equilibrium model results first proposed by Storti et al.[13] In a $\gamma_{\mathrm{II}} \times \gamma_{\mathrm{III}}$ plane, this region corresponds to the square triangle shown in Fig. 2. Inside this square triangle, any (γ_{II}, γ_{III}) pair yields complete separation provided that the constraints on γ_{I} and γ_{IV} are not violated. Figure 2 also shows the true region of complete separation, which might be twisted leftward and downward and significantly reduced. The deformation is due to the non-linear equilibrium, as shown by the simulations of Mazzotti et al.,[5] Gentilini et al.,[6] and Migliorini et al.,[7] while the reduction is due to the non-ideal conditions, as shown by the simulation of Azevedo and Rodrigues.[8]

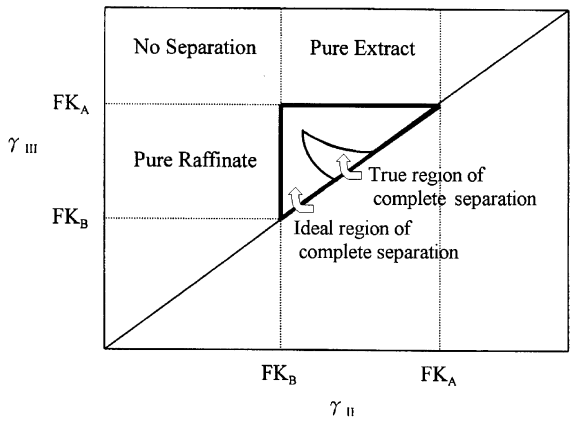

Figure 2. The ideal and true regions of complete separation in the $\gamma_{\mathrm{II}} \times \gamma_{\mathrm{III}}$ plane.

MARCEL DEKKER, INC.
270 Madison Avenue, New York, New York 10016

The liquid flow rates in a TMB process include the four internal liquid flow rates, Q_{I}, Q_{II}, Q_{III}, and Q_{IV} (or Q_{recycle}), and the four external flow rates, Q_F, Q_D, Q_E, and Q_R, which are related by the overall mass balances at the nodes of the four sections. Therefore, there are only four independent variables among them, and Q_F, Q_D, Q_E (or Q_R), and Q_{recycle} are usually set during the process. The four liquid flow rates, together with the solid flow rate (Q_s), have to be properly chosen based on the constraints of Eq. (1). Since both SMB and TMB systems have similar cyclic steady-state performance, the estimated TMB operating conditions can be applied to SMB. The switch time t_s in the SMB operation can be calculated from the solid velocity of TMB by $u_s = L_c/t_s$, where L_c is the length of the column. The liquid velocities or flow rates v_j^* or Q_j^* of SMB in four sections are evaluated by $v_j^* = v_j + u_s$ or $Q_j^* = Q_j + Q_s/F$.

The quick method for finding the region of good separation can be referred to our previous study.[9] First, a TMB flow rate optimization strategy, proposed by the "triangle theory" with linear and ideal conditions considered as explained above, is used to develop a complete separation region. The only parameters that need to be provided are the equilibrium Henry's constants of each isomer, which are measured using the elution chromatographic method.[14–16] Then, the eight-column SMB experiments are run with operating conditions selected around the complete separation region. Finally, the optimal operating conditions and separation performances are found based on the experimental results.

Process Performance Parameters

The SMB performance is characterized by four process parameters: purity, recovery, solvent consumption, and adsorbent productivity. Table 1 defines the process performance parameters for the case of binary separation, in which the less retained species B is recovered in the raffinate and the more retained species A is recovered in the extract.

EXPERIMENTAL

Columns and Chemicals

The chiral columns of Pirkle covalent *D*-phenylglycine were purchased from Regis (Morton Grove, IL). They included one analytical column of 25.0 cm L × 0.46 cm ID and 5 μm in particle diameter and eight semi-preparative columns of 10.0 cm L × 1.0 cm ID and 10 μm in particle diameter. (*R*)-(+)-1-1′-bi-2-naphthol (*R*-form, 99% pure, formula weight 286.33),

Marcel Dekker, Inc.
270 Madison Avenue, New York, New York 10016

Table 1. Simulated moving-bed process performance parameters.

Performance parameters	Extract	Raffinate
Purity (%)	$\frac{\overline{C_{AE}}}{(\overline{C_{AE}}+\overline{C_{BE}})}$	$\frac{\overline{C_{BR}}}{(\overline{C_{BR}}+\overline{C_{AR}})}$
Recovery (%)	$\frac{Q_E\overline{C_{AE}}}{Q_F C_{AF}}$	$\frac{Q_R\overline{C_{BR}}}{Q_F C_{BF}}$
Solvent consumption (mL/mg)	$\frac{(Q_F+Q_D)}{Q_E\overline{C_{AE}}}$	$\frac{(Q_F+Q_D)}{Q_R\overline{C_{BR}}}$
Productivity (mg/min)	$Q_E\overline{C_{AE}}$	$Q_R\overline{C_{BR}}$

Note: $\bar{C}$: Time averaged concentration ($0 \sim t_s$); Q: flow rate. Subscripts: A: more-retained species; B: less-retained species; E: extract; R: raffinate; F: feed; D: eluent.

(*S*)-(−)-1-1′-bi-2-naphthol (*S*-form, 99% pure, formula weight 286.33), 1-1′-bi-2-naphthol (racemic mixture, 99% pure, formula weight 286.33), and 1,3,5-tri-tert-butyl benzene (TTBB, 99%, formula weight 246.44) were purchased from Aldrich (Milwaukee, WI). HPLC grade hexane and IPA were purchased from Tedia (Fairfield, OH).

Analytical Chromatographic System

The high performance liquid chromatograph (HPLC) system included a Jasco Model PU-980 solvent metering pump, a Jasco Model UV-970 UV detector (Tokyo, Japan), a Rheodyne Model 7125 6-way syringe loading valve fitted with a 20 μL sample loop (Cotati, CA), and a Sunway Model 940-CO column oven (Taipei, Taiwan). The millivolt signal from the detector was converted to digital form with the aid of an analog-to-digital interface card (Scientific Information Service Corp., Taiwan) interfaced with a microcomputer for data storage and processing.

Measurement of the Adsorption Characteristics and Bed Porosity

The adsorption characteristics and bed porosity of each of the eight semi-preparative columns (10.0 cm L × 1.0 cm ID and 10 μm) used at each of the solvent compositions (hexane/IPA = 90/10, 80/20, 70/30) were measured

MARCEL DEKKER, INC.
270 Madison Avenue, New York, New York 10016

using the elution chromatographic method[14–16] and the previously described HPLC system.

Measurement of the Solubility Limit

The solvent composition has a great effect on the solubility limit of the racemic mixture. The solubility limit at each of the solvent compositions (hexane/IPA = 90/10, 80/20, 70/30) was measured by the following procedure. First, at each solvent composition, the over-saturated solution of the racemic mixture was prepared and shaken in a water bath of 30°C for several hours. Then, the clear supernatant of the upper layer of each solution was collected and analyzed by liquid chromatography under analytical conditions. Finally, the concentration, i.e., the solubility limit, of the racemic mixture at each solvent composition was calculated by the linear calibration graph of concentration versus peak area.

Simulated Moving-Bed Laboratory Unit

Figure 3 shows the eight-column laboratory scale SMB system. It consisted of eight semi-preparative columns of 10.0 cm L × 1.0 cm ID arranged in a 1-1-1-1 configuration, i.e., two columns per section. The fluid stream coming out of the fourth section was collected in a storage flask and recycled back to section I, which formed a closed-loop configuration. All the columns were located in a water bath, the temperature of which was controlled at 30°C.

As shown in Fig. 3, five flows (feed, eluent, extract, raffinate, and recycled eluent) had to be handled in the unit. The two inlet streams (feed and eluent) were controlled by two MPLC pumps (SSI Series III, USA). The two outlet streams (extract and raffinate) were controlled by two flow meters (AALBORG, NY). The flow rate of the fluid stream coming out of the fourth section was determined by the overall mass balance of the SMB unit, and the recycled eluent coming out of the storage flask was controlled by one MPLC pump (SSI Series III). Five electropneumatic 12-port multiposition valves (VICI-Valco EMTCSD12UW, Schenkon, Switzerland) were controlled by a computer to actuate the SMB. One valve was connected to the feed port, one to the solvent port, one to the raffinate port, one to the extract port, and the last one to the recycle port. The movement of each valve was controlled using V-PD-MICROEA software (VICI-Valco). The T joints at the top and bottom of each column allowed them to be connected in series, or to a recycling line. To avoid backmixing, check valves were placed on the lines connecting each column to the following one. All the lines in the unit made of stainless steel had 0.50 mm ID.

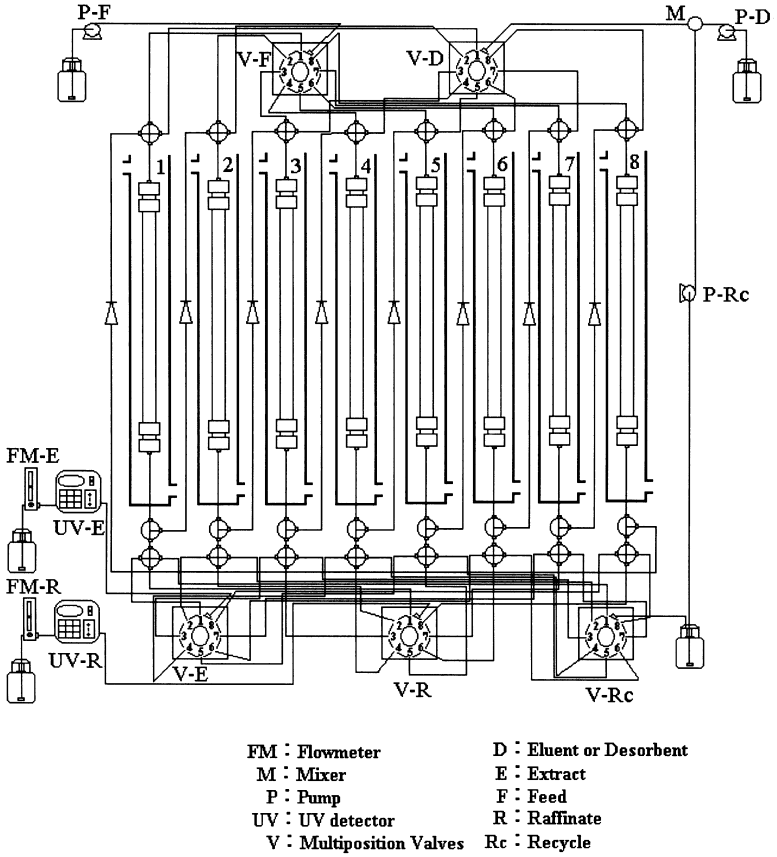

Figure 3. Scheme of the eight-column SMB laboratory unit.

Two ISCO Retriever 500 fraction collectors (Lincoln, NE) were used to collect the samples of the two outlet streams, i.e., extract and raffinate, for each cycle. The concentration and purity of each sample were analyzed on the analytical chiral column (25.0 cm L × 0.46 cm ID and 5 μm) using the standard analytical chromatographic system described above. The absorbance wavelength was set at 254 nm. Meanwhile, two UV spectrophotometric detectors (Jasco UV-970 with a preparative cell), both operating at 347 nm, were connected to the SMB unit as shown in Fig. 3. They were located on the extract line, between the extract position valve and the extract flow meter, and on the raffinate line, between the raffinate position valve and the raffinate flow meter, respectively. They monitored the concentration histories at these two ports.

MARCEL DEKKER, INC.
270 Madison Avenue, New York, New York 10016

RESULTS AND DISCUSSION

Effect of Solvent Compositions on the Adsorption Characteristics and Solubility Limit

The adsorption characteristics of the eight 10-cm columns used at each of the three solvent compositions (hexane/IPA = 90/10, 80/20, 70/30) were measured for both isomers. They included the retention factor (or Henry's constant) of each of the isomers (K_R and K_S), the separation factor (α), and the column efficiency (or the number of theoretical plates) of each isomer (N_R and N_S). The average results of the eight columns at each solvent composition are listed in Table 2. Table 2 also shows the solubility limits measured for the three solvent systems. It is noted that, with increasing solvent IPA concentration, the retention factor of each isomer decreased and the solubility limit increased significantly, but the column efficiency and the separation factor were about the same. In general, the relative standard deviations (RSD) of the column efficiencies of the two isomers were larger, which means that the column efficiency was much less reproducible than the other column parameters. The low average value of the separation factor, $\alpha = 1.20$–1.30, suggests that separation of the two isomers was difficult to perform with the SMB unit.

The average total bed porosity (ε) of the eight columns, measured at the solvent composition of 70/30 hexane/IPA using TTBB (nonadsorbable on the chiral column), was found to be 0.697 with 0.358% RSD.

Arrangement of the Experimental Runs

Using the average values of the total bed porosity and retention factors shown in Table 2, the square triangle regions of complete separation in the $\gamma_{II} \times \gamma_{III}$ plane, formed by the flow constraints proposed by the linear and ideal model, for the three different solvent systems were plotted as shown in Fig. 4. The complete separation regions were then used to select the proper operating conditions for the three solvent systems. Table 3 shows the six sets of experimental runs performed with the following operating conditions: solvent composition, hexane/IPA; liquid flow rates, Q_F, Q_D, Q_E, Q_R, and Q^*_{recycle}; switch time, t_s; generalized flow rate ratios, γ_j; j = I, II, III, IV. Three cases of the solvent composition (hexane/IPA = 90/10, 80/20, 70/30), two cases of the feed flow rate ($Q_F = 0.2$ and 0.3 mL/min), and three cases of the feed concentration of the racemic mixture ($C_F = 2.29$, 4.50, and 6.75 mg/mL) were considered. The feed concentration was restricted by the limit of solubility as shown in Table 2. The Q_E, Q_R, and Q^*_{recycle} values and the sum of the flow rates of the inlet/outlet streams, i.e., the $Q_F + Q_D = Q_E + Q_R$ value (=2.5 mL/min),

MARCEL DEKKER, INC.
270 Madison Avenue, New York, New York 10016

Table 2. The average adsorption characteristics of the semi-preparative columns used and the solubility limits at the three solvent compositions.

Solvent composition (hexane/IPA)	K_R[a] (RSD%[c])	K_S[a] (RSD%[c])	α (RSD%[c])	N_R[b] (RSD%[c])	N_S[b] (RSD%[c])	Solubility limit (mg/mL)
90/10	3.710 (0.98%)	2.961 (1.43%)	1.252 (1.31%)	3801 (3.59%)	3593 (4.33%)	2.55
80/20	2.009 (1.07%)	1.629 (1.54%)	1.234 (1.38%)	3688 (3.83%)	3534 (4.47%)	7.09
70/30	1.412 (1.13%)	1.128 (1.65%)	1.253 (1.43%)	3658 (3.95%)	3405 (4.72%)	10.11

[a]Unit: mL of solution/mL of adsorbent.
[b]Flow rate: 4.0 mL/min.
[c]RSD (relative standard deviation)% $= \dfrac{\text{standard deviation}}{\text{average}} \times 100\%$.

MARCEL DEKKER, INC.
270 Madison Avenue, New York, New York 10016

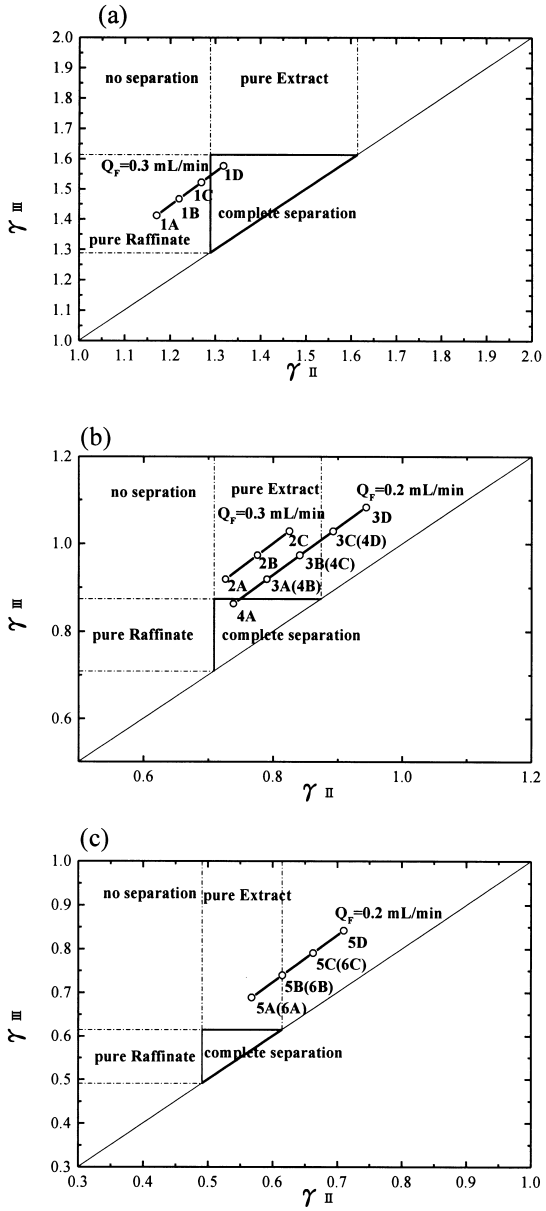

Figure 4. Location of the operating points of the experimental runs (operating conditions are referred to Table 3) in the $\gamma_{II} \times \gamma_{III}$ plane: (a) 90/10 hexane/IPA solvent; (b) 80/20 hexane/IPA solvent; (c) 70/30 hexane/IPA solvent.

MARCEL DEKKER, INC.
270 Madison Avenue, New York, New York 10016

Table 3. Operation conditions of the experimental runs ($Q_F + Q_D = 2.5$ mL/min).

Set no.	Run no.	Solvent (hexane/IPA)	t_s (min)	C_F (mg/mL)	Q_F (mL/min)	Q_D (mL/min)	Q_E (mL/min)	Q_R (mL/min)	$Q^*_{recycle}$ (mL/min)	γ_I	γ_{II}	γ_{III}	γ_{IV}
1	1A	90/10	4.4	2.29	0.3	2.2	1.1	1.4	1.6	2.0543	1.1702	1.4113	0.28603
	1B		4.5	2.29	0.3	2.2	1.1	1.4	1.6	2.1237	1.2195	1.4661	0.31525
	1C		4.6	2.29	0.3	2.2	1.1	1.4	1.6	2.1931	1.2688	1.5209	0.34448
	1D		4.7	2.29	0.3	2.2	1.1	1.4	1.6	2.2626	1.3181	1.5757	0.37371
2	2A	80/20	3.5	2.29	0.3	2.2	1.1	1.4	1.6	1.4296	0.72627	0.91808	0.022976
	2B		3.6	2.29	0.3	2.2	1.1	1.4	1.6	1.4990	0.77559	0.97288	0.052204
	2C		3.7	2.29	0.3	2.2	1.1	1.4	1.6	1.5684	0.82492	1.0277	0.081432
3	3A	80/20	3.5	2.29	0.2	2.3	1.1	1.4	1.6	1.4935	0.79021	0.91808	0.022976
	3B		3.6	2.29	0.2	2.3	1.1	1.4	1.6	1.5647	0.84136	0.97288	0.052204
	3C		3.7	2.29	0.2	2.3	1.1	1.4	1.6	1.6360	0.89251	1.0277	0.081432
	3D		3.8	2.29	0.2	2.3	1.1	1.4	1.6	1.7072	0.94365	1.0825	0.11066
4	4A	80/20	3.4	4.50	0.2	2.3	1.1	1.4	1.6	1.4223	0.73906	0.86328	0.006252
	4B		3.5	4.50	0.2	2.3	1.1	1.4	1.6	1.4935	0.79021	0.91808	0.022976
	4C		3.6	4.50	0.2	2.3	1.1	1.4	1.6	1.5647	0.84136	0.97288	0.052204
	4D		3.7	4.50	0.2	2.3	1.1	1.4	1.6	1.6360	0.89251	1.0277	0.081432
5	5A	70/30	3.3	4.50	0.2	2.3	1.1	1.4	1.4	1.2305	0.56735	0.68791	0.002932
	5B		3.4	4.50	0.2	2.3	1.1	1.4	1.4	1.2980	0.61484	0.73906	0.004893
	5C		3.5	4.50	0.2	2.3	1.1	1.4	1.4	1.3656	0.66234	0.79021	0.005912
	5D		3.6	4.50	0.2	2.3	1.1	1.4	1.4	1.4332	0.70983	0.84136	0.006175
6	6A	70/30	3.3	6.75	0.2	2.3	1.1	1.4	1.4	1.2305	0.56735	0.68791	0.002932
	6B		3.4	6.75	0.2	2.3	1.1	1.4	1.4	1.2980	0.61484	0.73906	0.004893
	6C		3.5	6.75	0.2	2.3	1.1	1.4	1.4	1.3656	0.66234	0.79021	0.005912

Note: Constraints for γ_I and γ_{IV}: hexane/IPA = 90/10: $\gamma_I > FK_R$ (1.613), $\gamma_{IV} < FK_S$ (1.287); hexane/IPA = 80/20: $\gamma_I > FK_R$ (0.873), $\gamma_{IV} < FK_S$ (0.708); hexane/IPA = 70/30: $\gamma_I > FK_R$ (0.614), $\gamma_{IV} < FK_S$ (0.490).

MARCEL DEKKER, INC.
270 Madison Avenue, New York, New York 10016

were fixed for all runs in the six sets. It is worth noting that none of the constraints on γ_I and γ_{IV} in each experiment were violated, as shown in Table 3.

Figure 4 also shows the location of the operating points of the experiments in the $\gamma_{II} \times \gamma_{III}$ plane, which is compared to that of the complete separation region. As can be seen in Table 3, the liquid flow rates in each of the six sets of experiments were kept constant, whereas the switch time was changed. This created a straight line in the $\gamma_{II} \times \gamma_{III}$ plane nearly parallel to the diagonal and cross or near the complete separation region, as shown in Fig. 4. The straight line moved away from the complete separation region as the feed flow rate increased. It is noted that, as the solvent composition changed from 90/10 to 70/30 hexane/IPA, the complete separation region in the $\gamma_{II} \times \gamma_{III}$ plane moved leftward and downward and its size was reduced, hence the feed flow rate had to be adjusted lower in order to let the experimental runs be located near the complete separation region.

Effect of Solvent Compositions on the Simulated Moving-Bed System Performance

The complete separation region of the $\gamma_{II} \times \gamma_{III}$ plane, developed under linear and ideal (axial dispersion and mass transfer resistance neglected) conditions, is only a reference for selecting proper operating conditions. The exact good separation region, when non-linearity and mass-transfer effects are present, has to be found experimentally.

The dynamic behavior of the SMB unit and the time needed to reach the periodic-steady state condition, were monitored based on the concentration and purity histories obtained at the extract and raffinate ports. Figure 5(a), (b) show the histories of the extract and raffinate concentrations, and Fig. 6(a), (b) show the histories of the averaged extract and raffinate purities of run 1C of the SMB system, respectively. It can be observed that the system took about six cycles (about 3.7 hours) to reach the periodic-steady state condition. The SMB was run for 10 cycles. In general, the time needed to reach the periodic-steady state condition was about 3.0–5.0 hours for all SMB runs.

Table 4 shows the experimental results obtained when the periodic-steady state of the SMB unit was reached. They are presented in terms of the steady state concentrations, optical purities, recoveries, product productivities, and solvent consumptions of the extract and raffinate streams. Based on the experimental results shown in Table 4, the effect of solvent compositions on the SMB performance were then examined.

For the first set, i.e., runs 1A–1D, the solvent composition used was 90/10 hexane/IPA. When the switch time was increased from 4.4 to 4.7 min, the experimental purity values, shown as a function of the switch time in Fig. 7(a),

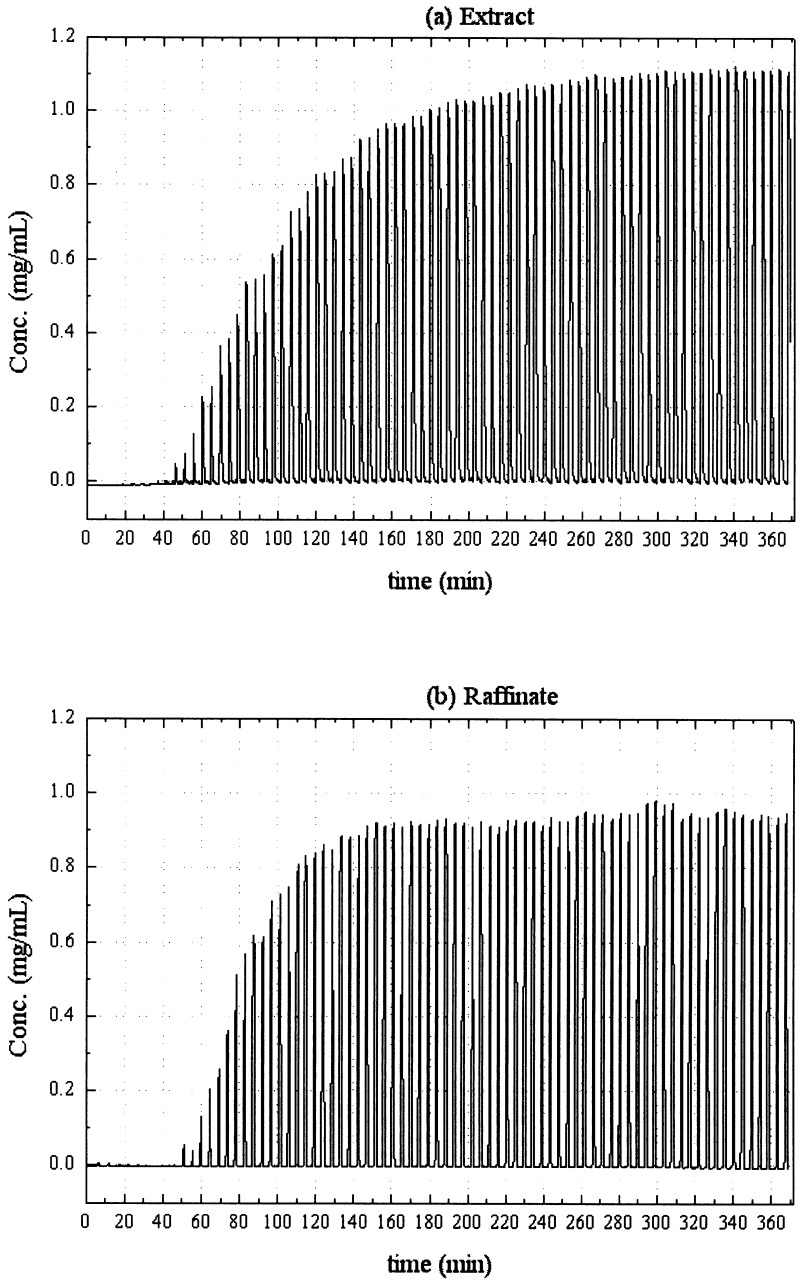

Figure 5. The histories of the extract and raffinate concentrations of Run 1C.

MARCEL DEKKER, INC.
270 Madison Avenue, New York, New York 10016

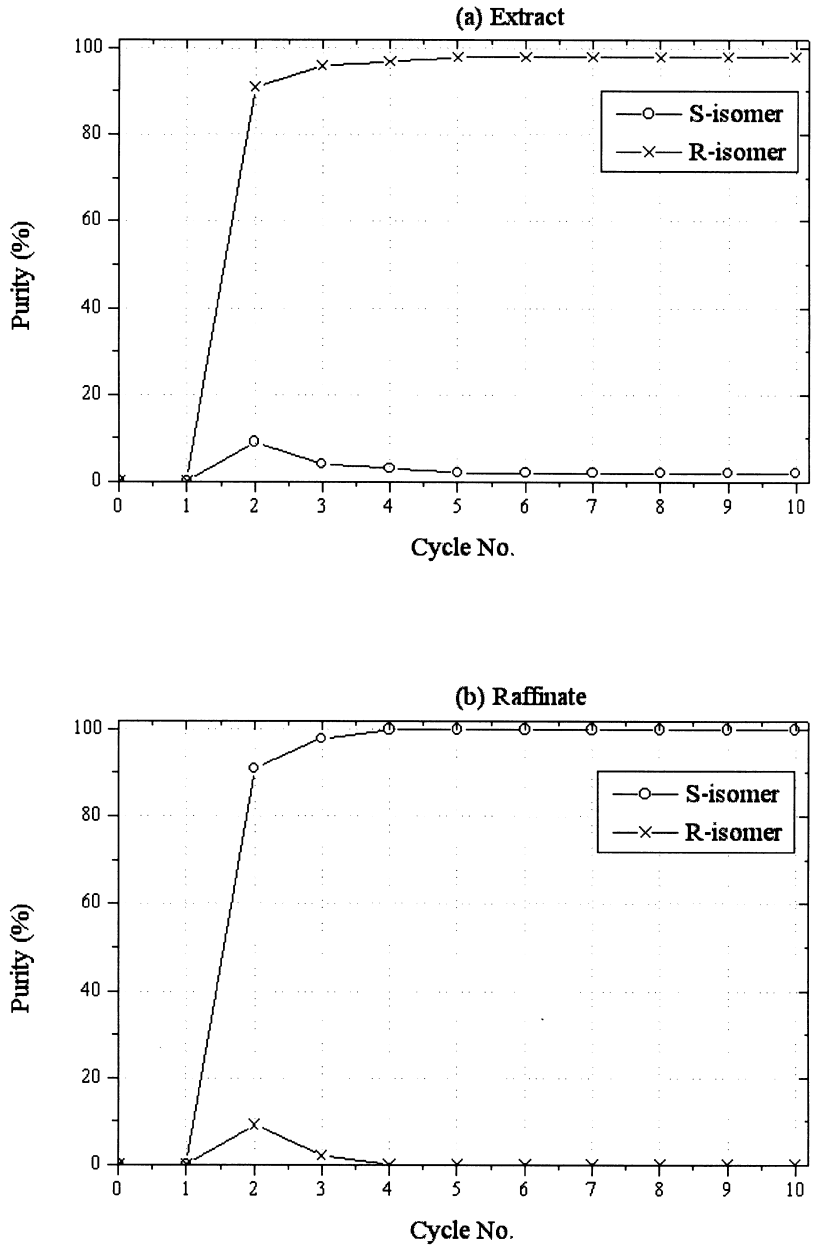

Figure 6. The histories of the averaged purities in each cycle of Run 1C.

MARCEL DEKKER, INC.
270 Madison Avenue, New York, New York 10016

Table 4. Separation performance of the SMB system.

Set no.	Run no.	Q_F[a]	C_F[b]	t_s[c]	P_A (%)	P_B (%)	$C_{E(A)}$[b]	$C_{E(B)}$[b]	$C_{R(A)}$[b]	$C_{R(B)}$[b]	$REC_{E(A)}$ (%)	$REC_{R(B)}$ (%)	$SOL_{E(A)}$[d]	$SOL_{R(B)}$[d]	$PRO_{E(A)}$[e]	$PRO_{R(B)}$[e]
1	1A	0.3	2.29	4.4	77	100	0.3125	0.0934	0.000	0.1722	100	70	7.27	10.37	0.344	0.241
	1B	0.3	2.29	4.5	95	100	0.3125	0.0164	0.000	0.2326	100	95	7.27	7.68	0.344	0.326
	1C	0.3	2.29	4.6	98	100	0.3125	0.0064	0.0000	0.2406	100	98	7.27	7.42	0.344	0.337
	1D	0.3	2.29	4.7	98	92	0.2859	0.0058	0.0210	0.2410	91	98	7.95	7.41	0.314	0.337
2	2A	0.3	2.29	3.5	88	100	0.3125	0.0426	0.0000	0.2121	100	86	7.272	8.420	0.344	0.297
	2B	0.3	2.29	3.6	98	98	0.3063	0.0063	0.0049	0.2407	98	98	7.420	7.420	0.337	0.337
	2C	0.3	2.29	3.7	97	67	0.1611	0.0050	0.1190	0.2417	52	98	14.111	7.389	0.177	0.338
3	3A	0.2	2.29	3.5	93	100	0.2084	0.0157	0.0000	0.1514	100	92	10.908	11.795	0.229	0.212
	3B	0.2	2.29	3.6	97	100	0.2084	0.0064	0.0000	0.1587	100	97	10.908	11.256	0.229	0.222
	3C	0.2	2.29	3.7	96	100	0.2084	0.0087	0.0000	0.1569	100	96	10.908	11.382	0.229	0.220
	3D	0.2	2.29	3.8	79	51	0.0109	0.0029	0.1550	0.1614	5	99	207.105	11.063	0.013	0.226
4	4A	0.2	4.50	3.4	82	99	0.4059	0.0891	0.0025	0.2514	99	78	5.600	7.102	0.446	0.352
	4B	0.2	4.50	3.5	97	99	0.4051	0.0125	0.0031	0.3116	99	97	5.610	5.731	0.446	0.436
	4C	0.2	4.50	3.6	97	98	0.4010	0.0124	0.0064	0.3117	98	97	5.668	5.729	0.441	0.436
	4D	0.2	4.50	3.7	83	58	0.1325	0.0271	0.2173	0.3001	32	93	17.152	5.950	0.146	0.420
5	5A	0.2	4.50	3.3	69	98	0.4045	0.1817	0.0037	0.1787	99	56	5.62	10.00	0.445	0.250
	5B	0.2	4.50	3.4	94	99	0.4052	0.0259	0.0030	0.3011	99	94	5.61	5.93	0.446	0.422
	5C	0.2	4.50	3.5	95	99	0.4052	0.0213	0.0031	0.3047	99	95	5.61	5.86	0.446	0.427
	5D	0.2	4.50	3.6	85	55	0.0869	0.0153	0.2531	0.3094	21	96	26.15	5.77	0.096	0.433
6	6A	0.2	6.75	3.3	85	96	0.5924	0.1045	0.0167	0.4000	97	83	3.83	4.46	0.652	0.560
	6B	0.2	6.75	3.4	95	98	0.6018	0.0317	0.0093	0.4573	98	95	3.78	3.91	0.662	0.640
	6C	0.2	6.75	3.5	93	88	0.5355	0.0403	0.0614	0.4505	87	93	4.24	3.96	0.589	0.631

Note: P, product purity; REC, recovery; SOL, solvent consumption; PRO, productivity. Subscripts: (A): R-isomer; (B): S-isomer; E: extract; R: raffinate; F: feed.
[a]mL/min; [b]mg/mL; [c]min; [d]mL/mg; [e]mg/min.

MARCEL DEKKER, INC. 270 Madison Avenue, New York, New York 10016

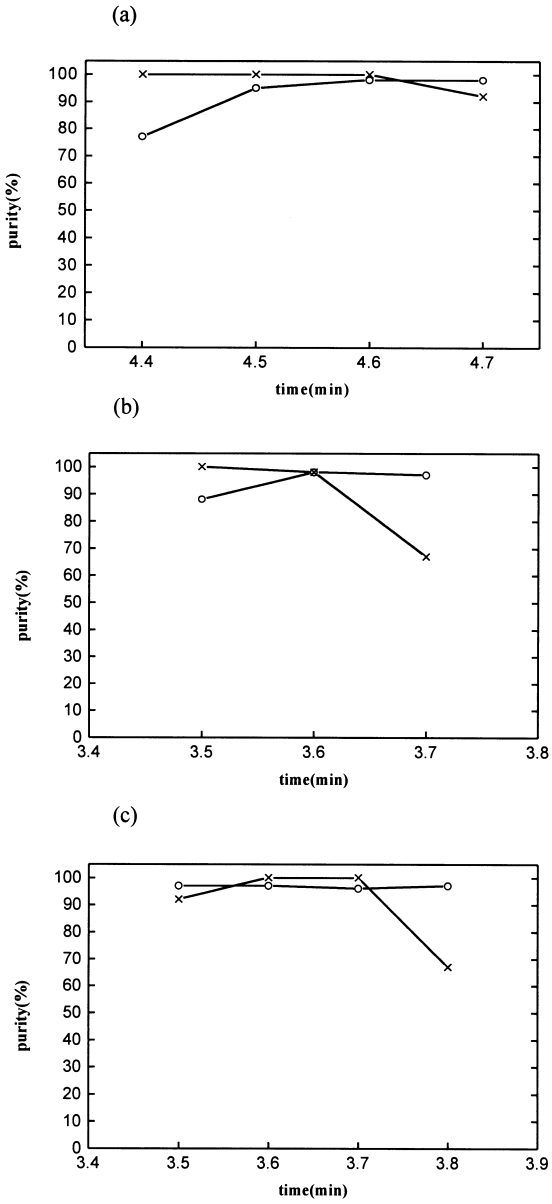

Figure 7. The optical purities of the extract and raffinate streams as a function of the switch time. (a) Set no. 1; (b) Set no. 2; (c) Set no. 3; (d) Set no. 4; (e) Set no. 5; (f) Set no. 6. –○–: *R*-isomer in the extract port; –×–: *S*-isomer in the raffinate port.

MARCEL DEKKER, INC.
270 Madison Avenue, New York, New York 10016

(d)

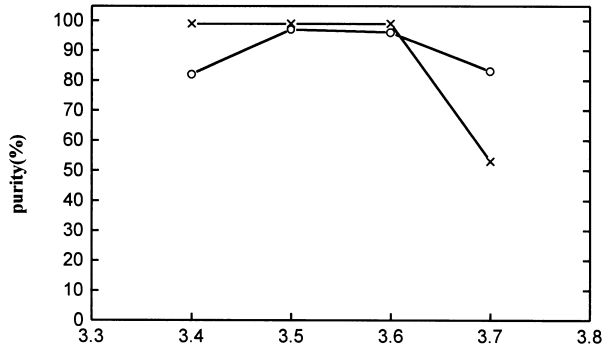

(e)

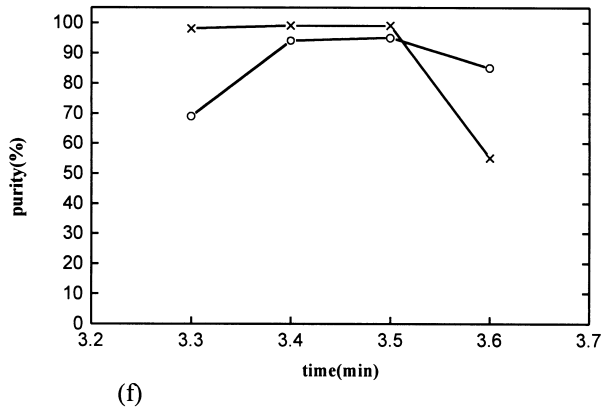

(f)

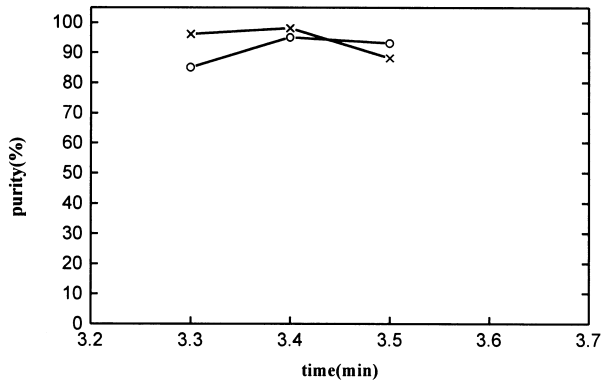

Figure 7. Continued.

MARCEL DEKKER, INC.
270 Madison Avenue, New York, New York 10016

exhibited the expected pattern of behavior; i.e., the raffinate purity decreased steadily while the extract purity increased from run 1A to run 1D. The best overall separation performance was achieved in run 1C, where the raffinate purity of 100% and the extract purity of 98% were obtained. It was hoped that the productivity (about 0.34 mg/min for each isomer) could be further increased with the increase in the feed flow rate or the feed concentration. However, the product purity could be reduced significantly by further increasing the feed flow rate, and the increase in the feed concentration was restricted by the limit of solubility of 2.55 mg/mL (Table 2) in the current solvent system.

For the second to fourth sets, the solvent composition used was 80/20 hexane/IPA and the limit of solubility can be increased to 7.09 mg/mL (Table 2). Using the same flow rate as in the first set ($Q_F = 0.3$ mL/min), the experimental purity values of the second set, i.e., runs 2A–2C, shown as a function of the switch time in Fig. 7(b), exhibited the same pattern of behavior as in the first set, but the range of operating conditions that led to the best product purity became smaller, i.e., the separation conditions became less robust. The robustness of the system operation was improved in the third set, where the feed flow rate was slightly reduced ($Q_F = 0.2$ mL/min). Figure 7(c) shows the experimental purity values of the third set, i.e., runs 3A–3D, as a function of the switch time. The range of operating conditions that led to the best product purity became larger and the best overall separation performance was achieved in run 3B, where the raffinate purity of 100% and the extract purity of 97% were obtained. However, due to the reduction in the feed flow rate, the productivity (about 0.22 mg/min for each isomer) was reduced to be about two thirds of that in the first set. The productivity was improved in the fourth set, where the feed concentration was increased two times ($C_F = 4.50$ mL/min). Figure 7(d) shows the experimental purity values of the fourth set, i.e., runs 4A–4D, as a function of the switch time. The comparison of Fig. 7(c), (d) shows that the product purity was about the same, but that the optimal switch time decreased slightly ($t_s = 3.5$ and 3.6 min in the fourth set as compared to $t_s = 3.6$ and 3.7 min in the third set), as the feed concentration increased from 2.29 mg/mL to 4.50 mg/mL. Since the variation in the feed concentration was not large, the effect of non-linear equilibrium was not very significant, and the productivity increased almost two times (about 0.44 mg/min for each isomer) to the increase in the feed concentration.

For the last two sets, the solvent composition used was 70/30 hexane/IPA and the limit of solubility can be further increased to 10.11 mg/mL (Table 2). Using the same feed flow rate and feed concentration as in the fourth set ($Q_F = 0.2$ mL/min and $C_F = 4.50$ mL/min), the experimental purity values of the fifth set, i.e., runs 5A–5D, shown as a function of the switch time in Fig. 7(e) were slightly reduced (the best extract purity reduced from 97% in the fourth set to 95% in the fifth set). This was due to the reduced size of the

MARCEL DEKKER, INC.
270 Madison Avenue, New York, New York 10016

good separation region in the current solvent system (Fig. 4). In order to further improve the productivity, the feed concentration was increased to $C_F = 6.75$ mL/min in the sixth set. Figure 7(f) shows the experimental purity values of the sixth set, i.e., runs 6A–6C, as a function of the switch time. The comparison of Fig. 7(e), (f) shows that, due to the significant effect of non-linear equilibrium under the high concentration condition, the range of operating conditions that led to the best product purity became very small, i.e., the separation conditions became very sensitive as the feed concentration increased from 4.50 mg/mL to 6.75 mg/mL. Therefore, the attempt of further improvement in the productivity was then hindered.

CONCLUSIONS

A quick experimental method has been used to achieve optimal operation of an SMB unit. Based on the experimental results of a series of SMB experiments, which were performed around the complete separation region proposed by the "triangle theory," the optimal operating conditions and separation performances were found. Using this method, optimization of an SMB unit was accomplished without the need for complicated mathematical models or tedious measurements of isotherm and kinetic parameters.

This method was used to study the effect of solvent compositions on the SMB performance. The results showed that solvent compositions had a significant influence on the system performance: the size of good separation region was reduced, but the feed concentration was increased with the solubility as the IPA percentage in the solvent increased. For the case of solvent composition of 90/10 hexane/IPA, the size of good separation region was large and the operation was stable, but the productivity tended to be lower because of the limitation of solubility. For the case of solvent composition of 70/30 hexane/IPA, due to the significant non-linear effect under the high concentration condition, the good separation region was twisted leftward and downward and its size was reduced. Although the feed concentration was increased significantly, the system performance was decreased. In comparison, the case of solvent composition of 80/20 hexane/IPA, due to its broad good separation region, stable operation, and high productivity, was considered as the best operating solvent composition of this system.

For our SMB system, under continuous separation of 1,1′-bi-2-naphthol enantiomers in the Pirkle *D*-phenylglycine chiral columns carried out in an eight-column SMB unit with a column length of 10 cm and using 80/20 hexane/IPA as eluent, good system performance (purity and recovery higher than 97% and productivity higher than 0.44 mg/min in each of the extract and raffinate ports) was achieved.

MARCEL DEKKER, INC.
270 Madison Avenue, New York, New York 10016

NOMENCLATURE

C	fluid-phase concentration, mg/mL of solution
F	phase ratio, $F=(1-\varepsilon)/\varepsilon$, mL of adsorbent/mL of solution
K_i	Henry's constant of species i, mL of solution/mL of adsorbent
L_c	column length, cm
L_j	zone length, cm
N_i	no. of theoretical plates of species i eluted in the CSP column
Q_j	external fluid flow rate and internal fluid flow rate in the TMB mode, mL/min
Q_j^*	internal fluid flow rate in the SMB mode, mL/min
Q_s	equivalent solid flow rate in the TMB mode, mL/min
t_s	switch time in the SMB mode, min
u_s	equivalent interstitial solid velocity in the TMB mode, cm/min
v_j	interstitial fluid velocity in the TMB mode, cm/min
v_j^*	interstitial fluid velocity in the SMB mode, cm/min
α	separation factor, $\alpha=K_A/K_B$
γ_j	ratio between the fluid and solid velocities in the TMB mode; $\gamma_j=v_j/u_s$
ε	column packing porosity

Subscripts

A	more retained species (R-isomer)
B	less retained species (S-isomer)
D	desorbent stream
E	extract stream
F	feed stream
i	isomer i, $i=R$-isomer (species A) or S-isomer (species B)
j	zone number, $j=$ I, II, III, IV
R	raffinate stream
recycle	recycle stream

ACKNOWLEDGMENT

The authors wish to thank the National Science Council of the Republic of China for financial support under grants NSC 89-2214-E-224-007 and NSC 90-2214-E-224-003.

MARCEL DEKKER, INC.
270 Madison Avenue, New York, New York 10016

REFERENCES

1. Broughton, D.B.; Gerhold, C.G. U.S. Patent 2,985,589, 1961.
2. Nicoud, R.M. LC-GC Int. **1992**, *5* (5), 43.
3. Stinson, S.C. Chem. Eng. News **1995**, *Oct. 9*, 44.
4. Balannec, B.; Hotier, G. *Preparative and Production Scale Chromatography*; Ganetsos, G., Barker, P.E., Eds.; Marcel Dekker, Inc.: New York, 1993.
5. Mazzotti, M.; Storti, G.; Morbidelli, M. J. Chromatogr. **1997**, *769*, 3.
6. Gentilini, A.; Migliorini, C.; Mazzotti, M.; Morbidelli, M. J. Chromatogr. **1998**, *805*, 37.
7. Migliorini, C.; Mazzotti, M.; Morbidelli, M. J. Chromatogr. **1998**, *827*, 161.
8. Azevedo, C.S.; Rodrigues, A.E. AIChE J. **1999**, *45* (5), 956.
9. Lai, S.-M.; Loh, R.R. J. Liq. Chromatogr. & Rel. Technol. **2002**, *25* (3), 345.
10. Pais, L.S.; Loureiro, J.M.; Rodrigues, A.E. AIChE J. **1998**, *44* (3), 561.
11. Ruthven, D.M.; Ching, C.B. Chem. Eng. Sci. **1989**, *44*, 1011.
12. Zhong, G.; Guiochon, G. Chem. Eng. Sci. **1996**, *51*, 4307.
13. Storti, G.; Mazotti, M.; Morbidelli, M.; Carra, S. AIChE J. **1993**, *39*, 471.
14. Miyabe, K.; Suzuki, M. AIChE J. **1992**, *38*, 6.
15. Lim, B.-G.; Ching, C.-B. Ind. Eng. Chem. Res. **1996**, *35*, 169.
16. Lai, S.-M.; Lin, Z.-C. Sep'n. Sci. & Tech. **1999**, *34* (16), 3173.

Received December 22, 2002
Accepted January 16, 2003
Manuscript 6054

MARCEL DEKKER, INC.
270 Madison Avenue, New York, New York 10016